

№ 15 (2015)

## Effects of Reduced Efficacy of KCC2 Co-Transporter in Single Neuron Model: Implications for Epilepsy

A. Yu. Buchin<sup>1</sup>, G. Huberfeld<sup>2</sup>, R. Miles<sup>3</sup>, A. V. Chizhov<sup>4</sup>, B.S. Gutkin<sup>5</sup>,  
V. Petrov<sup>6</sup>

<sup>1</sup>École Normale Supérieure, Paris, France, <sup>2</sup>Pierre and Marie Curie University, Paris, France, <sup>3</sup>Institut du Cerveau et de la Moelle Epiniere, Paris, France, <sup>4</sup>Ioffe Physical Technical Institute of the Russian Academy of Sciences, St. Petersburg, Russia, <sup>5</sup>NRU Higher School of Economics, Moscow, Russia, <sup>6</sup>Peter the Great St. Petersburg Polytechnic University, Russia

### Эффекты уменьшения активности хлорно-калиевого ко-транспортера KCC2 в модели единичного нейрона: приложения для эпилепсии

А. Ю. Бучин<sup>1</sup>, Ж. Хуберфельд<sup>2</sup>, Р. Майлс<sup>3</sup>, А. В. Чижов<sup>4</sup>, Б. С. Гуткин<sup>5</sup>,  
В. М. Петров<sup>6</sup>

<sup>1</sup>Высшая нормальная школа, Париж, Франция, <sup>2</sup>Университет Пьера и Марии Кюри, Париж, Франция, <sup>3</sup>Институт головного и спинного мозга, Париж, Франция, <sup>4</sup>Физико-технический институт им. А. Ф. Иоффе РАН, Санкт-Петербург, Россия, <sup>5</sup>Национальный исследовательский университет «Высшая школа экономики», Москва, Россия, <sup>6</sup>Санкт-Петербургский политехнический университет Петра Великого, Россия

**Keywords:** epilepsy, KCC2, extracellular potassium, intracellular chloride.

Experimentally it has been found that around 20% of pyramidal cells in epileptogenic human subiculum do not have KCC2 co-transporter. This pathology leads to the increased chloride level in pyramidal cells, what changes the action of GABA synapses from inhibition to excitation. In this work we propose the single neuron biophysical model to explain the mechanisms of this pathology. We show that decreasing the activity of the KCC2 brings the cell to the continuous spiking regime associated with the seizure activity. Using a set of simplifications we show the minimal biophysical model capable of describing this effect. The model proposed in this work provides the explanation for KCC2 pathology in pyramidal cells found in the temporal lobe.

**Ключевые слова:** эпилепсия, KCC2, внеклеточный калий, внутриклеточный хлор.

Экспериментально было обнаружено, что около 20% пирамидных клеток в области человеческого субикулума не обладают хлорно-калиевым ко-транспортером KCC2. Данная патология приводит к увеличению концентрации хлора в таких нейронах, что увеличивает их возбудимость. В настоящей работе мы представляем биофизическую модель данной патологии и показываем, что уменьшение активности KCC2 может перевести активность нейрона в режим долговременной генерации спайков, характерный для эпилептических приступов. Используя серию упрощений мы находим минимальную биофизическую модель, способную описать данный эффект. Предлагаемая минимальная модель позволяет объяснить патологию нейронов височной коры, связанную с отсутствием KCC2 ко-транспортера у пирамидных клеток.

## 1. Introduction

Epilepsy is one of the most common neurological disorders. Despite the fact that there is a lot of research in the field, about 40% of patients do not respond to medication [1]. In the latter case the only treatment is the surgical removal of the tissue with the epileptogenic focus. This tissue could provide the key insights into the mechanisms of epilepsy. Experimentally it has been found that about 20% of pyramidal cells in the epileptogenic human subiculum do not have functional KCC2 co-transporter [2]. In the normal conditions this molecule is responsible for maintaining the baseline chloride homeostasis in neurons of the central nervous system [3, 4]. Changes in the neuronal concentration induced by the intense activation of GABA-synapses could lead to the transition from inhibitory to excitatory neurotransmission [5, 6].

The KCC2 co-transporter is using the ion gradient created by the sodium-potassium pump to transfer ions from the neurons to the extracellular space. During each cycle of activity, it transmits chloride and potassium ions into the extracellular space [7, 8]. Hereby the accumulation of the extracellular potassium due to the neural activity and KCC2 could lead to the pathologic increase in the excitability by the creation of the positive feedback loop between the neural activity and the extracellular potassium [9]. Thus the dynamics of both ions is important to maintain the physiological activity level.

In this work we study the pathology of the KCC2 co-transporter on the single neuron level. We show that changes of the KCC2 activity could switch the cell to the regime of the continuous spike generation for the tonic phase of the epileptic activity [7, 8]. The consequences of KCC2 pathology on the network level are studied in detail in our paper [3].

## 2. Material and Methods

*Pyramidal cell model:* The pyramidal cell consists of dendritic and somatic compartments coupled with the dendritic current. The dynamics of the membrane potential on both compartments is described using Hodgkin-Huxley type equations. It is assumed that the membrane potential is changed instantaneously due to the strong sodium and potassium currents [9]. The ion concentration is dynamic in the model and updates at each time step. The reversal potentials for potassium and chloride currents are calculated according to the Nernst equation. The model equations are described in the following way [7, 9]:

### Voltage on the Dendrite Compartment

$$C_m \frac{dV_D}{dt} = \sum_i I_{int}^i - g_C^D (V_D - V_S) + I_{Leak}^D$$

$$I_{Leak}^D = -G_{Cl}^L (V_D - V_{Cl}) - G_K^L (V_D - V_K) - G_{Na}^L (V_D - V_{Na})$$

$$\sum_i I_{int}^i = I_{Na_p} + I_{Na_D} + I_{KCa} + I_{Ca} + I_{Leak}^D + I_{Km} + I_{pump}^{NaK} + I_{syn}$$

### Voltage on Somatic Compartment

$$g_C^S (V_D - V_S) = \sum_i I_{int}^i + I_{Leak}^S$$

$$I_{Leak}^S = -g_{Cl}^L (V_S - V_{Cl}) - g_K^L (V_S - V_K) - g_{Na}^L (V_S - V_{Na})$$

$$\sum_i I_{int}^i = I_{Kv} + I_{Na} + I_{Leak}^S + I_{pump}^{NaK}$$

### Dynamic Reversal Potentials

$$V_K = \frac{RT}{F} \ln\left(\frac{K^+_{OUT}}{K^+_{IN}}\right) \quad V_{Na} = \frac{RT}{F} \ln\left(\frac{Na^+_{OUT}}{Na^+_{IN}}\right)$$

$$V_{Cl} = \frac{RT}{F} \ln\left(\frac{Cl^-_{IN}}{Cl^-_{OUT}}\right) \quad V_{GABA} = \frac{RT}{F} \ln\left(\frac{4Cl^-_{IN} + HCO_3^-_{IN}}{4Cl^-_{OUT} + HCO_3^-_{OUT}}\right)$$

### Sodium-Potassium Pump

$$A(K^+_{OUT}, Na^+_{IN}) = \frac{1}{(1 + K^+_{\alpha} / K^+_{OUT})^2} \frac{1}{(1 + Na^+_{\alpha} / Na^+_{IN})^3}$$

$$I_{Kpump} = -2I \max A(K^+_{OUT}, Na^+_{IN})$$

$$I_{Napump} = 3I \max A(K^+_{OUT}, Na^+_{IN})$$

$$I_{pump}^{NaK} = I_{Kpump} + I_{Napump}$$

### Dynamic Ion Concentration

$$dK^+_{OUT} / dt = (k_K / Fd)(\Sigma I_K^{int} + I_K^{pump} - I_{KCC2}) + G$$

$$G = \frac{k_{ON}}{k_{1N}}(B_{max} - B) - k_{OFF} K^+_{OUT} B$$

$$dB / dt = k_{ON}(B_{max} - B) - k_{OFF} K^+_{OUT} B$$

$$dCl^-_{IN} / dt = (k_{Cl} / F)(I_D^{Cl} + I_{GABA} + I_{KCC2})$$

$$I_{KCC2} = I_{KCC2}(V_K - V_{Cl}) / ((V_K - V_{Cl}) + V_{1/2}),$$

$$\Sigma I_K^{int} = g g_{kl}(V_S - V_K) + I_{Kv} / 200$$

$$I_D^{Cl} = G_{ID}(V_D - V_{Cl}) + g_I(V_D - V_{Cl})$$

$$\tau_{Cl} = \tau_{Cl0} + \frac{\tau_{Clinf}}{1 + \exp((Cl_{\infty} - K^+_{OUT}) / \tau_{Kocl})}$$

### Axo-Somatic Compartment

#### Delayed Rectifier K Current

$$I_{Kv} = G_{Kv} m_{iKv}(V_S - V_K)$$

$$\frac{dm_{iKv}}{dt} = -\frac{m_{iKv} - m_{iKv}^{\infty}}{\tau_{Kvm}}$$

$$\tau_{Kvm} = \frac{1}{a_{iKv} + b_{iKv}} \quad m^{\infty}_{Kv} = \frac{a_{iKv}}{a_{iKv} + b_{iKv}}$$

$$a_{iKv} = 0.02 \frac{V_S - 25}{1 - \exp(-(V_S - 25) / 9)} \quad b_{iKv} = -0.02 \frac{V_S - 25}{1 - \exp(-(V_S - 25) / 9)}$$

### Na Current

$$I_{Na} = G_{Na} m^3_{iNa} h_{iNa} (V_S - V_{Na})$$

$$\frac{dm_{iNa}}{dt} = - \frac{m_{iNa} - m_{\infty}}{\tau_m}$$

$$\frac{dh_{iNa}}{dt} = - \frac{h_{iNa} - h_{\infty}}{\tau_h}$$

$$am_{iNa} = 0,182 \frac{V_S + 25}{1 - \exp(-(V_S + 25) / 9)} \quad bm_{iNa} = 0,124 \frac{V_S + 7}{1 - \exp(-(V_S + 25) / 9)}$$

$$ah_{iNa} = 0,024 \frac{V_S + 40}{1 - \exp(-(V_S + 40) / 5)} \quad bh_{iNa} = 0,0091 \frac{V_S - 65}{1 - \exp(-(-V_S - 65) / 5)}$$

$$\tau_m = \frac{1}{am_{iNa} + bm_{iNa}} \quad \tau_h = \frac{1}{ah_{iNa} + bh_{iNa}} \quad m_{\infty} = \frac{am_{iNa}}{am_{iNa} + bm_{iNa}}$$

### Na Sensitive K Current

$$I_{NaK} = g_{NaK} (V_S - V_K)$$

$$g_{NaK} = G_{NaK} \frac{0,37}{(1 + (77,4 / Na^+_{iN})^{3,5})}$$

$$\frac{dh_{iNa}}{dt} = - \frac{h_{iNa} - h_{\infty}}{\tau_h}$$

### Dendrite Compartment

#### Na Current

$$I_{NaD} = G_{NaD} m^3_{iNaD} h_{iNaD} (V_D - V_{Na})$$

$$\frac{dm_{iNaD}}{dt} = - \frac{m_{iNaD} - m^{\infty}_{iNaD}}{\tau_{mD}}$$

$$\frac{dh_{iNaD}}{dt} = - \frac{h_{iNaD} - h^{\infty}_{iNaD}}{\tau_{hD}}$$

$$am_{iNa} = 0,182 \frac{V_D + 25}{1 - \exp(-(V_D + 25) / 9)} \quad bm_{iNa} = 0,124 \frac{V_S + 25}{1 - \exp(-(V_D + 25) / 9)}$$

$$ah_{iNa} = 0,024 \frac{V_D + 40}{1 - \exp(-(V_D + 40) / 5)} \quad bh_{iNa} = 0,0091 \frac{V_D - 65}{1 - \exp(-(-V_D - 65) / 5)}$$

$$\tau_{mD} = \frac{1}{2,9529(am_{iNaD} + bm_{iNaD})} \quad \tau_{hD} = \frac{1}{2,9529(ah_{iNaD} + bh_{iNaD})}$$

$$m_{iNaD}^{\infty} = \frac{am_{iNaD}}{am_{iNaD} + bm_{iNaD}} \quad h_{iNaD}^{\infty} = \frac{1}{1 + \exp((V_D + 55) / 6,2)}$$

$$\tau_{mD} = \frac{1}{2,9529(am_{iNaD} + bm_{iNaD})}$$

### High-Threshold Ca Current

$$I_{Ca} = G_{Ca} m_{Ca}^2 h_{Ca} (V_D - V_{Ca})$$

$$\frac{dm_{iHVA}}{dt} = -\frac{m_{iHVA} - m_{Ca}^{\infty}}{\tau_{Ca}^m}$$

$$\frac{dh_{iHVA}}{dt} = -\frac{h_{iHVA} - h_{Ca}^{\infty}}{\tau_{Ca}^h}$$

$$\tau_{Ca}^m = \frac{1}{am_{iHVA} + bm_{iHVA}} \quad \tau_{Ca}^h = \frac{1}{ah_{iHVA} + bh_{iHVA}}$$

$$m_{Ca}^{\infty} = \frac{am_{iHVA}}{am_{iHVA} + bm_{iHVA}} \quad h_{Ca}^{\infty} = \frac{ah_{iHVA}}{ah_{iHVA} + bh_{iHVA}}$$

$$am_{iHVA} = 0,055 \frac{-27 - V_D}{\exp((-27 - V_D) / 3,8) - 1}$$

$$bm_{iHVA} = 0,94 \exp((-75 - V_D) / 17)$$

$$ah_{iHVA} = 0,000457 \exp((-13 - V_D) / 50)$$

$$bh_{iHVA} = \frac{0,0065}{\exp((-V_D - 15) / 28 + 1)}$$

### Slowly Activating Potassium Current

$$I_{Km} = G_{Km} m_{Km} (V_D - V_K)$$

$$dm_{Km} / dt = (m_{Km} - m_{Km}^{\infty}) / \tau_{Km}$$

$$m_{Km}^{\infty} = (a_{Km}) / (a_{Km} + b_{Km})$$

$$\tau_{Km} = 1 / (a_{Km} + b_{Km}) / 2,9529$$

$$a_{Km} = 0,001(V_D + 30) / (1 - \exp(-V_D + 30) / 9))$$

$$b_{Km} = -0,001(V_D + 30) / (1 - \exp\{-V_D + 30\} / 9\})$$

**Ca-Activated K Current**

$$I_{KCa} = G_{KCa} m_{iKCa}^2 (V_D - V_K)$$

$$dm_{iKCa} / dt = (m_{iKCa} - m_{iKCa}^\infty) / \tau_{Ca}$$

$$m_{iKCa}^\infty = (48 / 0,03(Ca_{IN}^+)^2) / (48 / 0,03(Ca_{IN}^+)^2 + 1)$$

$$\tau_{Ca} = (1 / (0,03(48(Ca_{IN}^+)^2 / 0,03 + 1))) / 4,65$$

**Mixed Cation Current**

$$I_h = G_h m_{ih} (V_D - V_h)$$

$$\frac{dm_{ih}}{dt} = -\frac{m_{ih} - h_\infty}{38}$$

$$h_\infty = \frac{1}{1 + \exp((V_D + 82) / 7)}$$

**Na Persistent Current**

$$I_{NapD} = G_{NapD} m_{iNapD} (V_D - V_{Na})$$

$$\frac{dm_{iNapD}}{dt} = -\frac{m_{iNapD} - m_{iNapD}^\infty}{0,1992}$$

$$m_{iNapD}^\infty = \frac{0,02}{1 + \exp(-(V_D + 42) / 5)}$$

**Synaptic Currents**

$$I_{syn} = -G_{AMPA} g_E (V_D - V_{AMPA}) - G_{GABA} g_I (V_D - V_{Cl})$$

AMPA:

$$\tau_E^1 \tau_E^2 \frac{d^2}{dt^2} g_E + (\tau_E^1 + \tau_E^2) \frac{d}{dt} g_E + g_E = \frac{1 - g_E}{K(\tau_E^1, \tau_E^2)} \sum_i \delta(t - t_i)$$

GABA:

$$\tau_I^1 \tau_I^2 \frac{d^2}{dt^2} g_I + (\tau_I^1 + \tau_I^2) \frac{d}{dt} g_I + g_I = \frac{1 - g_I}{K(\tau_I^1, \tau_I^2)} \sum_i \delta(t - t_i)$$

$$K(a, b) = \frac{ab}{a-b} \left[ \left(\frac{a}{b}\right)^{\frac{b}{b-a}} - \left(\frac{a}{b}\right)^{\frac{a}{b-a}} \right]$$

**Parameters**

Active conductances:  $G_{NapD} = 3,5\text{mS/cm}^2$ ,  $G_{HVA} = 0,0195\text{mS/cm}^2$ ,

$G_{Na} = 3450\text{mS/cm}^2$ ,  $G_{NaD} = 1,1\text{mS/cm}^2$ ,  $G_{Km} = 0,01\text{mS/cm}^2$ ,

$G_{Kv} = 200\text{mS/cm}^2$ ,  $G_{KCa} = 2,5\text{mS/cm}^2$

*Passive conductances:*  $g^D_C = 0,60\text{mS/cm}^2$ ,  $g^S_C = 100\text{mS/cm}^2$ ,

$g^L_K = 0,042\text{mS/cm}^2$ ,  $g^L_{Na} = 0,0198\text{mS/cm}^2$ ,  $G^L_K = 0,044\text{mS/cm}^2$ ,

$G^L_{Cl} = 0,01\text{mS/cm}^2$ ,  $G^L_{Na} = 0,02\text{mS/cm}^2$

*Synaptic conductances:*  $G_{AMPA} = 2\text{mS/cm}^2$ ,  $G_{GABA} = 3\text{mS/cm}^2$

*Sodium-potassium pump:*  $I^S_{\max} = 25\mu\text{A/cm}^2$ ,  $I^D_{\max} = 25\mu\text{A/cm}^2$

*Membrane capacitance:*  $C_m = 0,75\mu\text{F/cm}^2$

*Ion concentrations:*  $Cl^-_{OUT} = 130\text{mM}$ ,  $K_i = 150\text{mM}$ ,  $K^+_{\alpha} = 3,5\text{mM}$ ,

$Na^+_{\alpha} = 20\text{mM}$ ,  $K^+_{Th} = 15\text{mM}$ ,  $B_{\max} = 500\text{mM}$ ,  $Na^+_{OUT} = 130\text{mM}$ ,

$Na^+_{IN} = 20\text{mM}$

*Reversal potentials:*  $V_{AMPA} = 0\text{mV}$ ,  $V_{Ca} = 140\text{mV}$

*Constants:*  $k_K = 10\ 1000\text{cm}^3$ ,  $k_{Cl} = 100\ 1000\text{cm}^3$ ,  $d = 0,15\text{m}$ ,

$F = 96489\text{C/mol}$ ,  $R = 8,31\text{J/mK}$ ,  $D_{Ca} = 0,85\text{cm}^2\text{mM}/\mu\text{A}$ ,

$k_{off} = 0,0008\text{mM}^{-1}\text{ms}^{-1}$ ,  $k_1 = 1\text{mM}^{-1}$ ,  $k_{OFF} = 1\text{mM}^{-1}$

*Time constants:*  $\tau_{Ca} = 300\text{ms}$ ,  $\tau^1_E = \tau^2_E = 5,4\text{ms}$ ,  $\tau^1_I = 0,1\text{ms}$ ,  $\tau^1_I = 8,3\text{ms}$

Single neuron parameters are taken to present the standard pyramidal neuron from [9], synaptic parameters are taken from [10] to describe the synaptic conductances received by the neuron during the extracellular stimulation.

**Simulations:** All numerical results are done in the program XPPAUT 7.0 (<http://www.math.pitt.edu/~bard/xpp/xpp.html>). The bifurcation analysis of the model is implemented using AUTO package. All simulations were carried out with the numerical step equal to 0,05 ms using the 4<sup>th</sup> order Runge-Kutta method. We ensured the stability of the numerical results by comparing with the smaller time steps.

## 3. Results

### 3.1. Minimal Neuron Model with Dynamic Ion Concentrations

We describe the following pathways of ion dynamics in the model, Fig. 1. The extracellular potassium concentration is determined by the activity of the delayed-rectifier potassium channel activated during spike generation, sodium-potassium pump, astrocytic glial buffer, and the KCC2 co-transporter. The intracellular chloride concentration is determined by the chloride leak current, GABA synaptic current and the activity of the KCC2. Both ion concentrations affect the reversal potential of potassium and GABA currents.

To describe the single neuron dynamics we take the existing model of the pyramidal neuron [9] and simplify it. The original model consists of 14 dif-

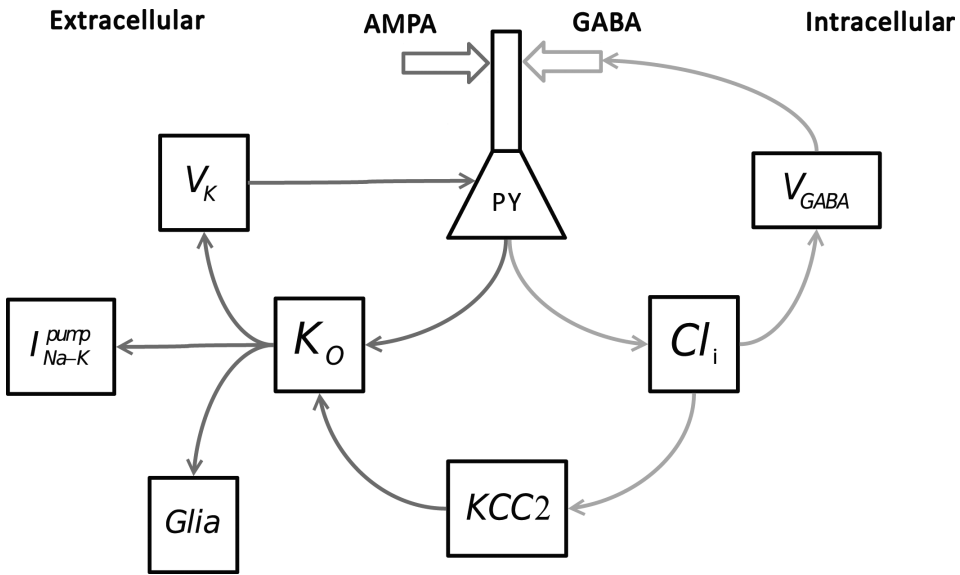


Fig. 1. Scheme of ion connections in the biophysical model. PY – pyramidal cell, AMPA, GABA — ampaergic and gabaergic synapses,  $K^+_{Out}$  — extracellular potassium concentration,  $Cl^-_{In}$  — intracellular chloride concentration,  $V_k$  — potassium reversal potential,  $V_{GABA}$  — gabaergic reversal potential,  $I^{pump}_{Na-K}$  — sodium-potassium pump, KCC2 — potassium-chloride co-transporter

ferential equations and describes the effect of multiple ionic currents on the dendrite and somatic compartments. In order to find the most important parameters we reduce the model to 4 differential equations. In this simplified model we describe only sodium and delayed-rectifier potassium as active currents responsible for the spike generation. The model also has multiple leak currents, including sodium, potassium and chloride ions. The derived minimal model has biophysical interpretation, whereas it is significantly simpler and amenable to the rigorous mathematical analysis.

The KCC2 co-transporter contributes to the ion concentration of potassium and chloride. The intracellular potassium and extracellular chloride are kept fixed, since their concentrations are very large [8]. In order to ensure that this approximation makes sense, we performed additional simulations with dynamic extracellular chloride and intracellular potassium (results not shown).

Since ion concentration changes are slow compared to the activity of sodium and potassium currents during the spikes, we use fast-slow decomposition and consider them as a parameter in the bifurcation analysis. We performed this analysis for simplified and full models, Fig. 2 A, B. Then we matched the excitability regions between these models by changing the dendrite potassium leak conductance. We managed to obtain a good qualitative accordance between the excitability area of the full and simplified models, Fig. 2 B, C.



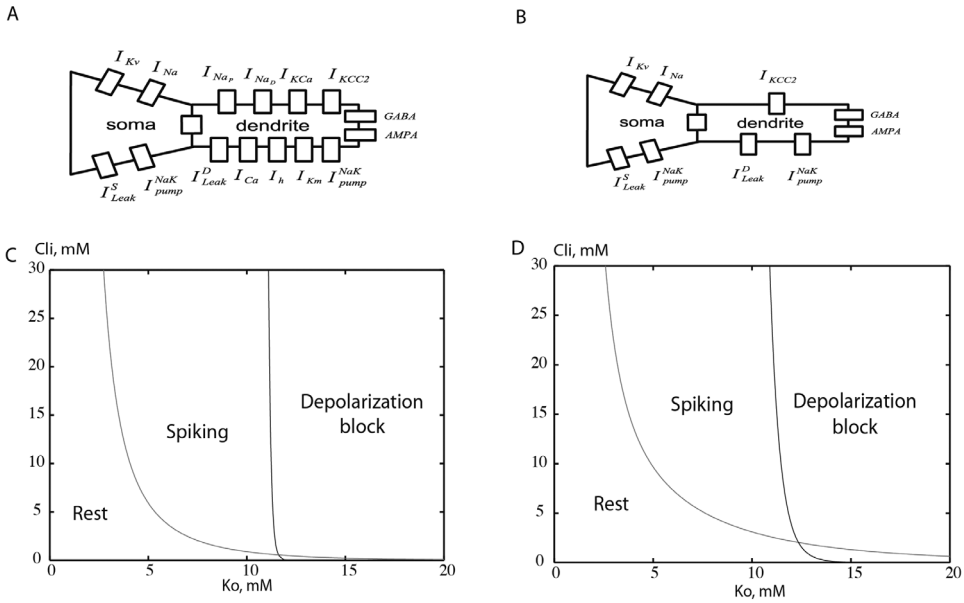


Fig. 2. Comparison of the full and simplified model.

- A, B – the scheme of the full and simplified models with intrinsic currents.
- C, D – bifurcation diagram of the full and simplified models for intracellular chloride and extracellular potassium.
- Red line – saddle-node bifurcation, black line – Andronov-Hopf bifurcation

### 3.2. Effect of Reducing Activity of the KCC2 Co-Transporter

In the derived simplified model we consider the effect of reducing the activity of the KCC2 co-transporter. To study the functional effect of this pathology we reduce the extrusion speed via the KCC2 co-transporter in the model. We define  $\tau_{Cl0} = 100$  ms for the normal cell and  $\tau_{Cl0} = 1000$  ms for the pathological cells. We should admit that the reduction in the speed of chloride extrusion is a reasonable model for our purpose, because the complete absence of KCC2 leads to the constant chloride concentration, which is not physiologically realistic [6, 11].

In order to model the synaptic input received by the neuron, we use the model of extracellular synaptic stimulation from [10, 12] to qualitatively reproduce the experimental conditions from [13]. In this experimental setup neurons are extracellularly stimulated in the epileptogenic slice derived after the brain biopsy. In this experiment the stimulation has triggered the generation of the pathologic activity from the activity focus in the slice, characteristic for the tonic phase of the epileptic activity.

We model the excitatory and inhibitory synaptic conductances received by the neuron during the extracellular stimulation. Each time when the synaptic stimulus is applied to the neuron, it generates a burst of spikes, Fig. 3 C, D. This leads to the increase in the extracellular potassium due to spiking and intracellular chloride due to the GABA input. The accumulation of these ions

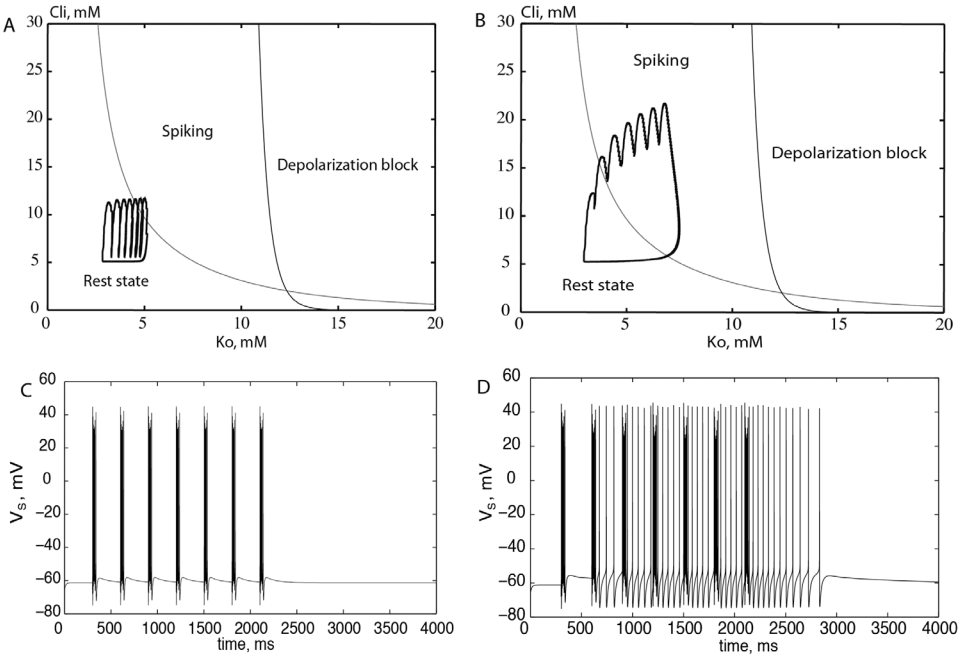


Fig. 3. Behavior of the model in the case of norm (A, C) and pathology (B, D) when stimulated by the periodic synaptic stimuli.

A, B – trajectory of the model in the phase space of chloride and potassium in the case of KCC2 norm ( $\tau_{Cl0} = 100$  ms) and pathology ( $\tau_{Cl0} = 1000$  ms).

C, D – the corresponding voltage trajectories.

Each burst of spikes corresponds to synaptic stimulation

brings the model to the spiking region on the state diagram, Fig. 3 A, B. When the model trajectory is in this region, it starts generating spikes caused by the increased concentration of potassium and chloride. In the case of KCC2 norm the model quickly moves to the baseline level of ion concentrations due to KCC2, sodium-potassium pump and glial buffer activity. In the case of KCC2 pathology due to the decreased chloride extrusion rate, the same synaptic stimulation leads to higher concentration of potassium and chloride. This brings the neuron to the spiking state for a longer period of time. In the latter case the model continues generating spikes, even in the absence of the synaptic stimuli, Fig. 3 B, D.

We should admit that spikes are possible in this model due to the synaptic stimulation or due to the increased ion concentration. This results from the fact that the phase space of the model is 4-dimensional, while in Fig. 3 A, B presents only a 2-dimensional projection. This diagram is not fully applicable to the analysis of the dynamics during the synaptic stimulation. But it precisely describes the model behavior on the slow time scale of ion dynamics after the synaptic stimulation.

### 3.3. Remark

In this work we presented the basic mechanism of KCC2 pathology found in pyramidal cells of human subiculum. The detailed model of this pathology

on the network level, as well as the comparison with the experimental data, is presented in the following work [3].

#### 4. Conclusions

Thereby based on the presented results we form the following conclusions:

1) The excitability area of the full biophysical model could be well approximated by the proposed simplified model in terms of the bifurcation diagram for the extracellular potassium and intracellular chloride parameters.

2) Reduction of the chloride extrusion due to the KCC2 co-transporter provokes generation of persistent spiking activity in response to synaptic stimulation due to the accumulation of the intracellular chloride and extracellular potassium.

**Acknowledgement.** This work has been supported by the following grants, Boris S. Gutkin: ANR-10-LABX-0087 IEC, ANR-10-IDEX-0001-02 PSL; Anatoly Buchin: ANR-10-LABX-0087 IEC, ANR-10-IDEX-0001-02, FRM FDT20140930942; Richard Miles and Gilles Huberfeld: ERC-322721. Theoretical part of this work was done at the National Research University Higher School of Economics Moscow and supported by Russian Federation government contract RFMEFI60815X0001. We would like to thank Maxim Bazhenov, Giri Krishnan and Sergei Prokhorenko for fruitful discussions.

#### REFERENCES

1. Beghi, E., Berg, A., Carpio, A., Forsgren, L., Hesdorffer, D.C., Hauser, W.A., Malmgren, K., Shinnar, S., Temkin, N., Thurman, D., & Tomson, T. Comment on epileptic seizures and epilepsy: definitions proposed by the International League Against Epilepsy (ILAE) and the International Bureau for Epilepsy (IBE). *Epilepsia*, 2005, 46(10), 1698–1699.
2. Huberfeld, G., Wittner, L., Clemenceau, S., Baulac, M., Kaila, K., Miles, R., & Rivera, C. Perturbed chloride homeostasis and GABAergic signaling in human temporal lobe epilepsy. *The Journal of neuroscience*, 2007, 27(37), 9866–9873.
3. Buchin, A., Chizhov, A., Huberfeld, G., Miles, R., & Gutkin, B. (in press) Reduced efficacy of the KCC2 co-transporter promotes epileptic oscillations in subiculum network model. *Journal of Neuroscience*.
4. Jedlicka, P., Deller, T., Gutkin, B.S., & Backus, K.H. Activity-dependent intracellular chloride accumulation and diffusion controls GABA(A) receptor-mediated synaptic transmission. *Hippocampus*, 2011, 21(8), 885–898.
5. Khalilov, I., Dzhala, V., Ben-Ari, Y., & Khazipov, R. Dual role of GABA in the neonatal rat hippocampus. *Developmental neuroscience*, 1999, 21(3–5), 310–319.
6. Rivera, C., Voipio, J., Payne, J.A., Ruusuvuori, E., Lahtinen, H., Lamsa, K., Privola, U., Saarna, M., & Kaila, K. The K<sup>+</sup>/Cl<sup>-</sup> co-transporter KCC2 renders GABA hyperpolarizing during neuronal maturation. *Nature*, 1999, 397(6716), 251–255.
7. Krishnan, G.P., & Bazhenov, M. Ionic dynamics mediate spontaneous termination of seizures and postictal depression state. *The Journal of Neuroscience*, 2011, 31(24), 8870–8882.
8. Bazhenov, M., Timofeev, I., Steriade, M., & Sejnowski, T.J. Potassium model for slow (2–3 Hz) in vivo neocortical paroxysmal oscillations. *Journal of neurophysiology*, 2004, 92(2), 1116–1132.

9. Mainen, Z.F., & Sejnowski, T.J. Influence of dendritic structure on firing pattern in model neocortical neurons. *Nature*, 1996, 382(6589), 363–366.
10. Chizhov, A.V. Conductance-based refractory density model of primary visual cortex. *Journal of computational neuroscience*, 2014, 36(2), 297–319.
11. Blaesse, P., Airaksinen, M.S., Rivera, C., & Kaila, K. Cation-chloride cotransporters and neuronal function. *Neuron*, 2009, 61(6), 820–838.
12. Chizhov, A.V. A model for evoked activity of hippocampal neuronal population. *Biophysics*, 2002, 47(6), 1086–1094.
13. Huberfeld, G., de la Prida, L.M., Pallud, J., Cohen, I., Le Van Quyen, M., Adam, C., Clemenceau, S., Baulac, M., & Miles, R. Glutamatergic pre-ictal discharges emerge at the transition to seizure in human epilepsy. *Nature neuroscience*, 2011, 14(5), 627–634.

---

**Anatoly Yu. Buchin**

Ecole Normale Supérieure, Laboratoire des Neurosciences Cognitives,  
Group for Neural Theory.

E-mail: anat.buchin@gmail.com

**Gilles Huberfeld**

PhD

Université Pierre et Marie Curie, Pitié-Salpêtrière Hospital, Neurophysiology Department,  
principal investigator.

E-mail: gilles.huberfeld@mac.com

**Richard Miles**

PhD

Institut du Cerveau et de la Moelle Épineuse, Cortex et Epilepsie Group,  
principal investigator.

E-mail: richard.miles@upmc.fr

**Anton V. Chizhov**

Ph.D. (Physical and Mathematical Sciences)

Ioffe Physical Technical Institute of the Russian Academy of Sciences,  
Computational Physics Laboratory,  
principal investigator.

E-mail: anton.chizhov@mail.ioffe.ru

**Boris S. Gutkin**

PhD

NRU Higher School of Economics, Center for Cognition and Decision Making,  
professor.

E-mail: boris.gutkin@gmail.com

**Victor M. Petrov**

Dr.Sc. (Physical and Mathematical Sciences)

Peter the Great St. Petersburg Polytechnic University, Institute of Physics,  
Nanotechnology and Telecommunications,  
head of Department of Quantum Electronics.

E-mail: vikpetroff@mail.ru